Journal of Molecular Catalysis A: Chemical 294 (2008) 93–101

Contents lists available at ScienceDirect

Journal of Molecular Catalysis A: Chemical

journal homepage: www.elsevier.com/locate/molcata

Modeling extra framework aluminum (EFAL) formation in the zeolite ZSM-5 using parametric quantum and DFT methods

Orlando Lisboa, Morella Sánchez, Fernando Ruette*

Laboratorio de Química Computacional, Centro de Química, IVIC, Apartado 21827, Caracas 1020-A, Venezuela

ARTICLE INFO

Article history:
Received 23 January 2008
Received in revised form 6 August 2008
Accepted 9 August 2008
Available online 19 August 2008

Keywords:
Zeolite
EFAL
CATIVIC
Parametric quantum method
Dealumination
Catalytic modeling

ABSTRACT

Quantum-chemical calculations were performed using the DFT method and a qualitative parametric quantum method (PQM) named CATIVIC, in order to model the whole EFAL formation process. Two clusters ($AlSi_3O_{12}H_9$ and $AlSi_{63}O_{152}H_{49}$) were employed to model zeolite ZSM-5. Formation of intermediate Al species was reported with four to zero bond coordinations to the zeolite framework. The EFAL formation process was analyzed by the evaluation of bond distances, diatomic bond energies changes (ΔDBE) and Wiberg's indexes (WI) of Al–O bonds. Penta- and hexacoordinated intermediates were produced and free $Al(OH)_3$ and $Al(OH)_3(H_2O)_2$ EFAL species were formed from the small and big clusters, respectively. Comparisons with the DFT method permit establishing that CATIVIC or a well-parameterized PQM method can be used to understand zeolite changes under hydrothermal treatment.

1. Introduction

Zeolites can be used in many catalytic applications due to their stability and activity combined with a high selectivity. They have a wide range of industrial applications in the refining, petrochemical, molecular sieves, sorbents, green chemistry, animal feeding, and detergent industries [1–3]. The reactivity of zeolites depends on their Brønsted acidic properties as well as Lewis acidity. The neutralization of the net negative charge on the framework aluminum (FAL) atoms by protons leads to Brønsted acid sites and the corresponding catalytic activity. The Lewis acidity is believed to be generated by extraframework aluminum (EFAL) [4], formed by dealumination of FAL, in a non-tetrahedral environment as well. In general, dealumination is achieved via steaming or acid leaching with different thermal treatments. In other words, framework hydrolysis of Si–O–Al linkages can lead to aluminum losses from the framework that enhances the catalyst activity [5].

EFAL particles in zeolites have been characterized by using various experimental techniques. The local environment of Al has been characterized by ^{27}Al magic angle spinning (MAS)-NMR, the locations of their peaks in X-ray absorption spectra (XAS), and the presence of hydroxyl bands in IR spectra [6–14].

Bourgeat-Lami et al. [6], using Al MAS NMR spectroscopy in zeolite-beta, concluded that the aluminum state depends on the cation nature that compensates lattice negative charges. Aluminum atoms with non-tetrahedral coordination symmetry (e.g., octahedral) remains connected to the framework and may be reverted to their tetrahedral coordination sphere by ion exchange with cations like Na^+, K^+, and by adsorption of ammonia (i.e., $Al^{VI} \rightarrow Al^{IV}$ transformation). They also observed that proton introduction in the lattice disturbs FAL atoms coordination. In addition, the strained T–O–T bridge bonds (T = Si and Al) can be broken forming $TO_{4-n}(OH)_n$ sites (n = 1, 2, and 3) in the presence of water [6].

Remy et al. [10], using MAS NMR and XPS spectroscopy, studied a series of dealuminated H–Y Zeolites. ^{27}Al MAS NMR spectroscopy shows the presence of three types of Al in dealuminated samples: framework tetrahedral, non-framework octahedral, and a third type of Al that may be localized into the zeolite framework. XPS data indicate that three types of acid sites are formed upon ammonia adsorption on dealuminated zeolites.

A change in the aluminum coordination is observed by Omegna et al. [11] in H–Y zeolite and amorphous silica, not only after treatment with a base but also after thermal treatment. Under wet conditions aluminum atoms are susceptible to hydrolysis of Al–O bonds and become octahedral after coordination of water molecules. A simple thermal treatment is enough to remove the water coordinated to these aluminum atoms, returning them to a tetrahedral coordination.

Von Bokhoven et al. [12] used ^{27}Al MAS and MQ (multiple quantum) MAS NMR in order to determine the aluminum coordination in zeolite-beta as a function of the heat treatment used. They found that in the presence of water a framework tetrahedral aluminum

* Corresponding author. Tel.: +58 212 5041442; fax: +58 212 5041350.
E-mail address: fruette@ivic.ve (F. Ruette).

1381-1169/$ – see front matter © 2008 Elsevier B.V. All rights reserved.
doi:10.1016/j.molcata.2008.08.003

site eventually creates an octahedral aluminum in the acidic zeolite. Octahedral Al(VI) completely is reversed into a framework tetrahedral coordination after ammonia treatment at 100 °C. A severe steaming causes a complete hydrolysis of tetrahedral FALs and at least two distorted octahedral FAL are formed. These Al species, under certain conditions, lose bonds with the framework oxygen and may become mobile in the zeolite pores and migrate to the crystallites surface.

Bugaev et al. [13], using X-ray absorption near-edge structure (XANES) spectroscopy, described the local structure of tetrahedrally coordinated aluminum with three short Al–O bonds (1.71 Å) and one long Al–OH bond (1.91 Å) in the dehydrated H-mordenite. However, they also reported Al–O distances of about 2.15 Å that are assigned to distorted octahedrally coordinated Al.

Kunkeler et al. [14] proposed an active site formation mechanism for the MPV (Meerwein–Ponndorf–Verley) ketone reduction in zeolite-beta. They concluded that water facilitates the Al–O bond breaking in the Si–OH–Al zone by forming a silanol group (SiOH) and by a water O atom coordination to the Al atom.

Recent studies show that HZSM-5 zeolite can also undergo dealumination. Bao et al. [15], using XRD, XRF and ^{27}Al MAS NMR spectroscopy, reported formation of EFAL species after steaming. On the other hand, Costa Vayá et al. [16] also proposed the EFAL formation in HZSM-5 after washing with water, drying and calcination at 400 °C.

Several theoretical calculations have been utilized to describe the structure and catalytic properties of zeolites by using EFAL models. A combined solid-state NMR and theoretical calculations (DFT) were carried out by Li et al. in dealuminated HY zeolite supercage model [17]. They showed that there exists a Brønsted/Lewis acid synergy mechanism with $Al(OH)_3$ and $Al(OH)^{2+}$ species. Alternatively, Benco et al. [18] performed *ab initio* molecular dynamics simulation to study the dynamical behavior of EFAL particles $Al(OH)_3(H_2O)$ and $Al(OH)_3(H_2O)_3$ located in the main channel and cage of gmelinite. They found multiple proton exchange between the zeolite framework and the EFAL particle in a highly acidic zeolite leading to charge separation ($EFAL^{2+}$ plus $zeolite^{2-}$). Ruiz and collaborators [19] also used *ab initio* quantum mechanical methods to examine the transformation for tetrahedral to octahedral coordination, in aluminum complexes $[Al(OH)_x(H_2O)_{n-x}]^{3-x}$ ($n = 4$, 5, and 6). They concluded that transformations involving aluminum coordination number changes do not require large energies and that, for a neutral complex, the stable coordination numbers were 4 and 5.

Bhering et al. [20] carried out DFT calculations for ultrastable Y (USY) zeolite concerning the structure of some selected EFAL species (Al^{3+}, $Al(OH)^{2+}$, AlO^+, $Al(OH)_2{}^+$, AlO(OH), and $Al(OH)_3$. They found that AlO^+ and $Al(OH)_2{}^+$ prefer a bicoordination to oxygen atoms near the four-membered ring containing two framework aluminum atoms. Another works using the same EFAL model ($Al(OH)_2{}^+$) and USY zeolite were performed by Mota et al. [21] using $Si_4Al_2O_{10}H_{10}$ cluster and the onion approach employing a 102 atom cluster [22]. They concluded that the role of EFAL is to stabilize the conjugated base formed upon deprotonation by hydrogen bonding and nucleophilic interaction with the framework oxygen atoms. They discard the Brønsted/Lewis synergism and their results explain experimental results obtained by Biaglow et al. [23] for faujasites.

On the other hand, Lukinskas and Fărcaşiu [24] studied aluminum and dialuminum oxide clusters as models of extraframework aluminum species in the dissociation of H_2. They found that the existence of unsaturated Al clusters might be the explanation of EFAL effect in steamed zeolites.

It is experimentally known that the zeolite catalytic activity is primarily determined by their structure and the presence of EFAL species. However, the role and the way EFAL species are formed remain poorly understood. The catalytic activity enhancement has been associated with the presence of EFAL species. For this reason the dealumination process is fundamental in understanding the transformations that lead to stable, active, and selective zeolite catalysts. In this work a theoretical modeling of EFAL formation is carried out by studying water molecules interactions on the vicinity of an Al site of ZSM-5 zeolite. Different levels of theory were considered for studying the EFAL formation process with DFT and the CATIVIC methods.

This paper is organized as follows. In Section 2, a brief description of the methodology and cluster models employed here are presented. In Section 3, EFAL formation results are discussed based on bond distances, bond strengths and Al–O diatomic binding energy changes in each step after a water molecule interaction with the Al site. This analysis was performed for both small and big zeolite cluster models considering a graphical schematic explanation of each step and bond property values for intermediate species. In addition, a description of the resulting intermediates was carried out in some detail. Finally, a summary of the most important features and comments coming out from this work are presented in Section 4.

2. Methodology

All calculations were carried out by the quantum parametric method named CATIVIC [25] and some of them with Gaussian program [26] using the B3LYP functional with a 6-31+G(d,p) basis set. The former method is based on simulation techniques to mimic the total energy functional using parametric elementary functionals [27–29].

Atomic parameters for H, O, and Si were taken from Ref. [30]; those for Al were selected from Ref. [31]. Molecular parameters for O–H, O–O, and H–H bonds were obtained from Ref. [30] and other molecular parameters, Al–O, Al–H, Al–Si, Si–O, Si–Si, and Si–H, were obtained from previous works [31].

Bond strengths were evaluated using diatomic bond energies (DBE) and Wiberg's indexes (WI) [32] for aluminum ligands. The former tool allows the evaluation of the bond formation and bond breaking in kcal/mol for all interacting atoms. This technique is based on energy partition applied to the parametric method with the condition that the total bond energy is equal to the sum of DBEs [33]. Because CATIVIC is a qualitative method from the energetic point of view, the local changes (DBE changes for all Al–O bonds) can give a qualitative idea of the energy changes through the whole EFAL process.

The starting geometry of the substrate to build these clusters was obtained from a web site database [34]. Two different model sizes were considered: $AlSi_3O_{12}H_9$ and $AlSi_{63}O_{152}H_{49}$, as drawn in Fig. 1. The selection of a four-membered ring framework model for studying H_2O–Al interaction and EFAL formation is supported by Kunkeler et al. [14]. Other theoretical modeling works also select fourfold ring as model for adsorption of EFAL species [17,20–22]. They affirm that most probably rings to undergo transformation are those that are under strain. In both model clusters, hydrogen atoms were used to tie off the peripheral O atoms and to saturate them. These hydrogen atoms were optimized with the other atoms fixed, and then they were kept unchanged when the rest is optimized. Calculations were carried with full geometry optimization except for the terminal H atoms. In order to maintain the neutral zeolite framework, a charge-balance proton attached to a bridging oxygen Al–O–Si is included in each model. All calculations start with a H_2O molecule within the region around the Al atom between 1.8 and 2.3 Å. The assortment of the particular region for H_2O interaction

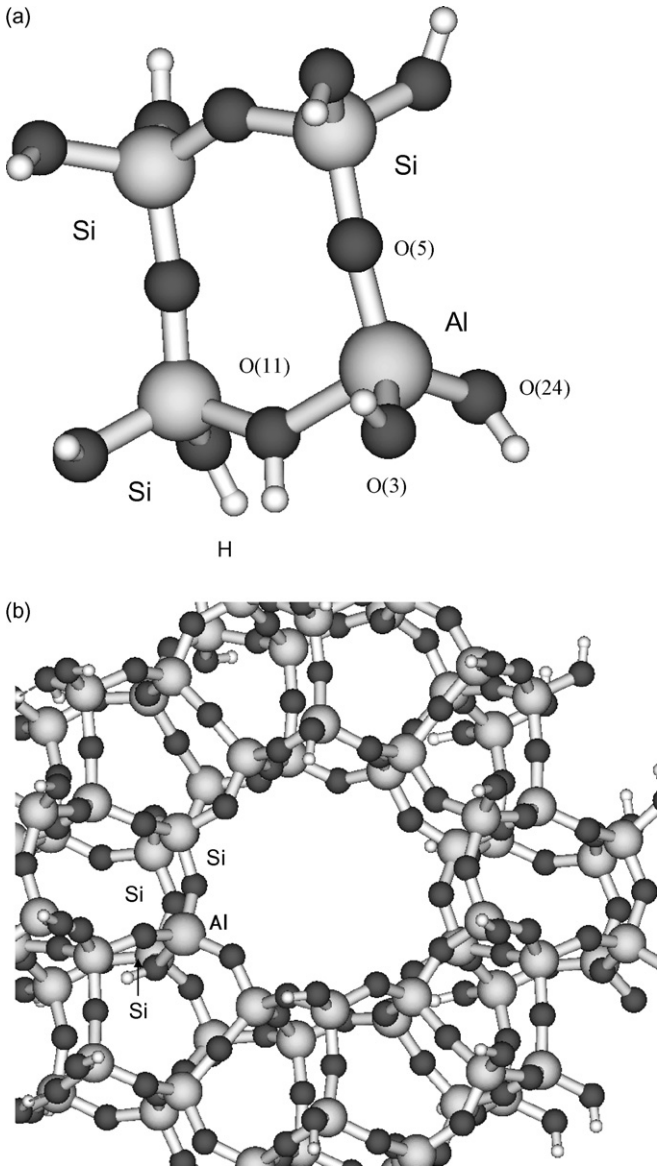

Fig. 1. Zeolite models for dealumination: (a) $AlSi_3O_{12}H_9$ and (b) $AlSi_{63}O_{152}H_{49}$.

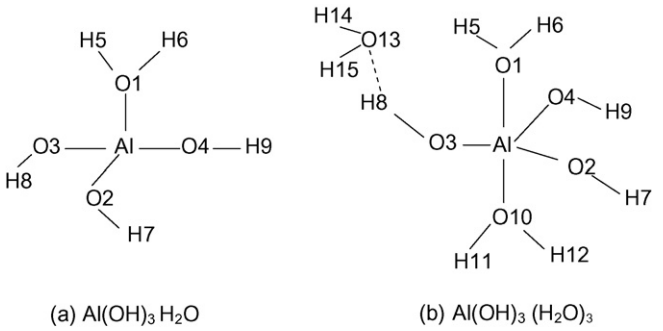

Fig. 2. Geometries of hexacoordinated ($Al(OH)_3(H_2O)_3$) and tetracoordinated ($Al(OH)_3H_2O$) aluminum species.

Table 1
Bond distances (Å) of $Al(OH)_3H_2O$ and $Al(OH)_3(H_2O)_3$ complexes from VASP* and CATIVIC methods (see Fig. 2)

Bond	$Al(OH)_3H_2O$		Bond	$Al(OH)_3(H_2O)_3$	
	CATIVIC	VASP		CATIVIC	VASP
Al–O(1)	2.01	2.00	Al–O(1)	2.11	2.049
Al–O(2)	1.74	1.726	Al–O(2)	2.12	2.136
Al–O(3)	1.74	1.725	Al–O(3)	1.76	1.782
Al–O(4)	1.74	1.724	Al–O(4)	1.76	1.747
O(1)–H(5)	0.95	0.977	O(1)–H(5)	0.95	0.979
O(1)–H(6)	0.95	0.976	O(1)–H(6)	0.95	0.981
O(2)–H(7)	0.93	0.965	O(2)–H(7)	0.93	0.974
O(3)–H(8)	0.93	0.965	O(3)–H(8)	0.93	0.966
O(4)–H(9)	0.93	0.965	O(4)–H(9)	0.93	0.962
			O(10)–H(11)	0.95	0.993
			O(10)–H(12)	0.95	0.974
			O(6)–H(14)	0.95	0.970
			O(6)–H(15)	0.95	0.970
			O(6)–H(11)	3.42	1.934
			Al–O(10)	2.12	2.136

* Values are given in Ref. [18].

in each step was selected according to the accessibility of the H_2O molecule.

In order to evaluate the precision of the CATIVIC method hexacoordinated ($Al(OH)_3(H_2O)_3$) and tetracoordinated ($Al(OH)_3H_2O$) aluminum species, as models of EFAL (see Fig. 2), were calculated and compared with the geometries obtained by Benco et al. [18] using a VASP simulation package [35]. Results presented in Table 1 indicate that there is a reasonable good correlation between CATIVIC and the VASP method.

3. Results and discussion

3.1. $AlSi_3O_{12}H_9$ model

In order to examine the CATIVIC performance, dealumination step calculations were also carried out for $AlSi_3O_{12}H_9$ (see Fig. 1a) by the DFT-B3LYP/6-31-G(p,d) method of Gaussian 98 [26]. Model cluster atom labels employed here are shown in Fig. 1a. Note that O(3), O(5), O(11), and O(24) are framework oxygen atoms in small

Table 2
Comparison in bond distance and time for CATIVIC with respect to DFT using the $AlSi_3O_{12}H_9$ cluster (see Fig. 1a).

Bond	Bond distances (Å)							
	$AlSi_3O_{13}H_{11}$[a]		$AlSi_3O_{14}H_{13}$[a]		$AlSi_3O_{14}H_{13}$[a]		$AlSi_3O_{15}H_{15}$[a]	
	CATIVIC	DFT	CATIVIC	DFT	CATIVIC	DFT	CATIVIC	DFT
Al–O(3)	1.84	1.76	1.87	1.77	1.90	1.79	4.32	3.43
Al–O(5)	1.82	1.73	1.84	1.75	1.87	1.80	1.85	1.77
Al–O(11)	2.08	1.98	2.25	2.17	4.73	3.41	4.75	3.37
Al–O(24)	1.84	1.73	1.85	1.76	1.89	1.79	1.85	1.76
Al–O(27)	–	–	2.34	2.17	2.17	2.05	2.27	2.02
Al–O(31)	–	–	–	–	2.11	2.11	2.23	2.06
Al–O(32)	–	–	–	–	–	–	1.84	1.84
Time (min)	1.93	11,940	1.78	14,580	2.50	24,840	5.37	40,980

[a] Cluster.

Table 3
Bond properties of intermediates using CATIVIC method. Bond distances (BD) and Wiberg's bond indexes (WI) (values in parentheses) in the formation of aluminum extraframework from $AlSi_3O_{12}H_9$ cluster (*)

Bond	Bond distances (Å) and (bond orders)						
	(a) $AlSi_3O_{12}H_9$	$1H_2O$ (b) $AlSi_3O_{13}H_{11}$	$2H_2O$ (c) $AlSi_3O_{14}H_{13}$	$3H_2O$ (d) $AlSi_3O_{15}H_{15}$	$4H_2O$ (e) $AlSi_3O_{16}H_{17}$	$5H_2O$ (f) $AlSi_3O_{17}H_{19}$	$6H_2O$ (g) $AlSi_3O_{18}H_{21}$
Al–O(3)	1.84 (0.72)	1.87 (0.68)	1.90 (0.64)	**4.32 (0.00)**	**4.41 (0.00)**	**5.16 (0.00)**	**8.28 (0.00)**
Al–O(5)	1.82 (0.66)	1.84 (0.65)	1.87 (0.63)	1.85 (0.64)	1.84 (0.69)	1.88 (0.61)	**8.91 (0.00)**
Al–O(11)	2.08 (0.30)	2.25 (0.22)	**4.73 (0.00)**	**4.75 (0.00)**	**4.97 (0.00)**	**5.21 (0.00)**	**11.40 (0.0)**
Al–O(24)	1.84 (0.67)	1.85 (0.65)	1.89 (0.63)	1.85 (0.66)	**4.83 (0.00)**	**5.16 (0.00)**	**11.15 (0.0)**
Al–O(27)		2.34 (0.16)	2.17 (0.23)	2.27 (0.19)	2.29 (0.17)	2.41 (0.13)	**6.57 (0.00)**
Al–O(31)			2.11 (0.22)	2.23 (0.19)	2.33 (0.16)	2.24 (0.19)	**8.02 (0.00)**
Al–O(32)				1.84 (0.67)	1.86 (0.66)	1.87 (0.66)	1.80 (0.78)
Al–O(35)					1.83 (0.67)	1.86 (0.62)	1.79 (0.78)
Al–O38)						2.41 (0.13)	**6.39** (0.00)
Al–O(41)							1.79 (0.78)
ΔDBE (kcal/mol)		−37.0	−3.1	2.7	8.4	−37.8	−143.2

Diatomic binding energy (DBE) change (ΔDBE) for each step is given in kcal/mol in the last row. (*) See Fig. 3. Bold values indicate Al-O broken bonds.

and big models. The O(11)–H corresponds to the bridging hydroxyl group in which the proton compensates the negatively charged aluminum.

Calculated Al–O bond distances (BD) are depicted in Table 2. Note that new oxygen atoms (O(27), O(31), O(32)) come from H_2O molecules bonded to Al as OH_2 and OH. In addition, all calculations show that Al–O bond distance values of the DFT method are smaller than those of the CATIVIC method. However, similar trends are observed, i.e., the same bonds are broken (BD > 2.5 Å) and formed (BD < 2.5 Å). One important issue is the computational time employed for modeling processes in both methods. Table 2 displays DFT computer times varying from about 8 days and 7 h to 28 days and 11 h, while in CATIVIC calculation time ranges from about 2 to 5.4 min. For that reason, the complete EFAL formation process is performed in this work with the CATIVIC method, using both $AlSi_3O_{12}H_9$ and $AlSi_{63}O_{152}H_{49}$ models.

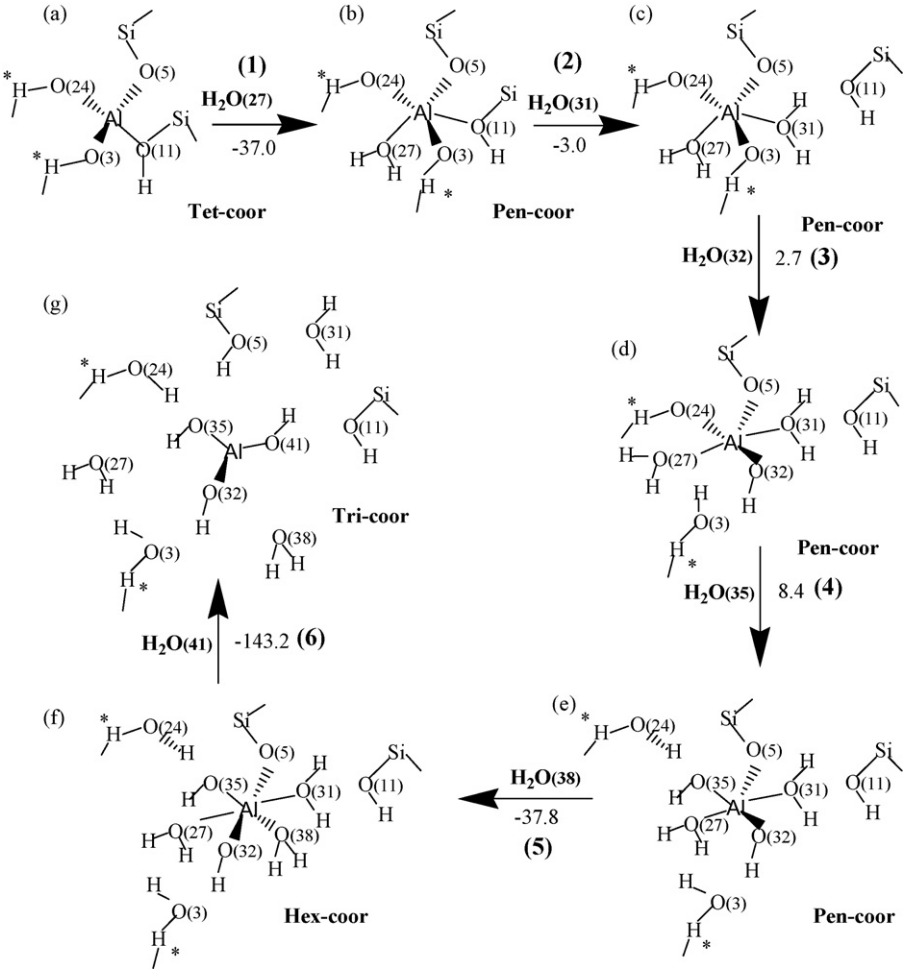

Fig. 3. Scheme of different steps in the EFAL formation process for the $AlSi_3O_{12}H_9$ model. (*) Means that those H atoms are kept fixed during the optimization procedure (see Fig. 1).

Calculations with CATIVIC were performed with the small cluster in order to understand the formation of H_2O–Al, HO–Al, and the breaking of Al–O and Si–O bonds. Part of the framework dealumination process for the $AlSi_3O_{12}H_9$ model was described in previous work [36]; however, in order to understand the H_2O–Al interaction in different steps until the formation of EFAL, results are presented in a scheme shown in Fig. 3 and in Table 3. Changes of DBE values for all Al–O bonds are also displayed in Table 3 and in Fig. 3, in order to analyze the main energetic change in each step of the process.

Results show that the addition of the first water molecule ($H_2O(27)$, step (1) in Fig. 3) leads to a species with a five-coordinated aluminum atom. This step is locally favored by an increase of 37 kcal/mol in the strength of all Al–O bonds ($\Delta DBE = -37$ kcal/mol) and the formation of a relatively weak O(27)–Al bond (BD = 2.34 Å and WI = 0.16). Note that an important change also occurs in the BD(Al–O(11)) from 2.08 to 2.25 Å and the corresponding WI from 0.30 to 0.22. This bond is the weakest in the $AlSi_3O_{12}H_9$ model, because O(11) contains an additional bond (O(11)–H), as shown in Fig. 3a. Penta-coordinated species have been experimentally reported by several authors [37–39] on different zeolites after steam treatment.

In the second step, another H_2O molecule ($H_2O(31)$, see Fig. 3c) is adsorbed and it causes the Al–O(11)H bond rupture. This result suggests that acidified water will favor EFAL formation, as recently reported by Marques et al. [8]. Bond properties values of Al–O(11), BD = 4.73 Å and WI = 0.00, confirm its bond breaking and Al–O(31)H_2 values of BD = 2.11 Å and WI = 0.22 indicate a relatively weak bond formation (see Table 3). A SiO–H bond formation also occurs, as shown in Fig. 3b. In this respect, Kiricsi et al. [40] reported internal SiOH groups at framework defects and SiOH terminal groups from the analysis of IR absorptions. Here, the other penta-coordinated species appears but with two water molecules and with three Al–O bonds to the zeolite framework.

A different process is observed with the addition of a third H_2O; the $H_2O(32)$ adsorption leads to SiO(3)–H bond formation and the Al–O(3) bond breaking (BD = 4.32 Å and WI = 0.00). Furthermore, the Al–O(32)H bond formation occurs (BD = 1.84 Å and WI = 0.67) (see Fig. 3d). In this sense, Wouters et al. [41] proposed that beside the framework dealumination a partial hydrolysis of Al–O bond occurs with the formation of Al–O–H species in the zeolite Y.

The adsorption of a forth water molecule ($H_2O(35)$, step (4)) produces the $H_2O(35)$–Al and H*O(24)–H bonds formation and the Al–O(24) bond breaking. This yields another penta-coordinated aluminum species attached to zeolite framework by only one Al–O(5)–Si bridge bond (Fig. 3e) with the Al bonded to two H_2O molecules and two OH groups.

A fifth water molecule ($H_2O(38)$) leads to a hexacoordinated species that has weak H_2O–Al bonds with a length of 2.41 Å and WI of 0.13 (see Table 3). This process releases energy ($\Delta DBE = -12.7$ kcal/mol) and the Al–O(x) (x = 3, 11, and 24) bond distances are increased. This last feature indicates that the Al site is moving away from the framework (see Fig. 3f and column (f) in Table 3). This octahedral coordinated species is experimentally supported by several authors [9–12,15,38,41,42].

Finally, the resulting EFAL after the attack of a sixth water molecule ($H_2O(41)$) produces a three-coordinated Al species that is very stable respect to the hexacoordinated one (see $\Delta DBE = -143.2$ kcal/mol in Table 3). The Al–O(5) bond is broken and Al–O(41)H is formed together with the SiO(5)–H bond. In this way an $Al(OH)_3$ compound is formed and all water molecules bonds to Al are broken ($H_2O(38)$–Al, $H_2O(31)$–Al, $H_2O(27)$–Al) after the interaction with $H_2O(41)$. Recently ^{1}H DQ MAS NMR experiments has revealed the existence of $Al(OH)_3$ species out of the framework [15], as previously suggested [43]. Threefold coordinated species have been also proposed at high temperature by Bugaev et al. [13]. The formation of $Al(OH)_3$ after steam dealumination has been schematically anticipated by Mota et al. [20] but with the interaction of three H_2O molecules instead of six ones, as found here. Results of the Al–O(x) optimized distances (x = 3, 5, 11, 24, 27, 31, and 38) indicate that the $Al(OH)_3$ molecule is moving far away from the zeolite framework and other H_2O molecules. Experimental results of Fleisch et al. [44] suggest that non-structural aluminum in faujasites migrates toward the zeolite particle surface after hydrothermally treated.

Note that this model is very simple and contains close to the Al reaction site fixed H* atoms that model the rest of the zeolite framework. In addition, the cage effect is not included into this model. Nevertheless, several interesting features were obtained from this elementary model.

3.2. $AlSi_{63}O_{152}H_{49}$ model

The process of framework zeolite dealumination is also analyzed considering a bigger model ($AlSi_{63}O_{152}H_{49}$) in order to see the effect of including the fourfold ring into a 10-fold ring channel, as shown in Fig. 1b. The atom labels are the same as those used in the $AlSi_3O_{12}H_9$ model. Note that in this cluster the H_2O molecules

Table 4
Bond distances (BD) and Wibergïs bond indexes (WI) (in parentheses) of intermediates (see Fig. 4 for species (a–i) in the formation of aluminum extraframework for $AlSi_{63}O_{152}H_{49}$ model, see Fig. 4

Bond	Bond distances (Å) and (Wiberg bond orders)								
	(a) $AlSi_{63}O_{152}H_{49}$	1H_2O (b) $AlSi_{63}O_{153}H_{51}$	2H_2O (c) $AlSi_{63}O_{154}H_{52}$	3H_2O (d) $AlSi_{63}O_{155}H_{54}$	4H_2O (e) $AlSi_{63}O_{156}H_{56}$	5H_2O (f) $AlSi_{63}O_{156}H_{56}$	6H_2O (g) $AlSi_{63}O_{157}H_{58}$	7H_2O (h) $AlSi_{63}O_{157}H_{58}$	8H_2O (i) $AlSi_{63}O_{158}H_{60}$
Al–O(3)	1.68 (0.68)	1.69 (0.67)	1.78 (0.64)	1.80 (0.59)	1.98 (0.31)	2.13 (0.26)	**2.56 (0.11)**	**3.20 (0.00)**	**3.02 (0.02)**
Al–O(5)	1.69 (0.65)	1.74 (0.61)	1.80 (0.61)	1.78 (0.64)	1.79 (0.62)	1.83 (0.57)	1.86 (0.57)	1.81 (0.59)	**3.25 (0.01)**
Al–O(11)	1.95 (0.31)	2.30 (0.18)	**3.82 (0.00)**	**4.38 (0.00)**	**4.55 (0.00)**	**4.89 (0.00)**	**5.18 (0.00)**	**5.27 (0.00)**	**5.49 (0.00)**
Al–O(24)	1.72 (0.61)	1.72 (0.61)	1.81 (0.60)	**3.17 (0.03)**	**3.71 (0.00)**	**4.73 (0.00)**	**4.71 (0.00)**	**4.96 (0.00)**	**4.95 (0.00)**
Al–O(27)		2.16 (0.19)	2.08 (0.23)	2.30 (0.15)	**3.40 (0.00)**	–	–	–	–
Al–O(31)			2.06 (0.23)	2.09 (0.21)	2.31 (0.17)	2.14 (0.21)	2.13 (0.21)	2.14 (0.21)	2.08 (0.23)
Al–O(32)				1.79 (0.64)	1.78 (0.61)	1.81 (0.60)	1.83 (0.59)	1.83 (0.59)	1.78 (0.62)
Al–O(35)					1.83 (0.53)	1.80 (0.60)	1.79 (0.62)	1.81 (0.63)	1.77 (0.63)
Al–O(38)						2.30 (0.14)	2.14 (0.19)	2.21 (0.18)	2.24 (0.19)
Al–O(41)							**2.68 (0.05)**	–	–
Al–O(44)								2.38 (0.14)	**5.2 (0.00)**
Al–O(47)									1.81 (0.61)
ΔDBE (kcal/mol)		−52.8	−8.5	13.4	16.5	14.0	−10.3	−12.7	85.8

Values of DBE changes (ΔDBE) for each step are shown in kcal/mol. All distance values greater than 2.5 Å are presented in bold together with its corresponding WI. Bold values indicate Al-O broken bonds.

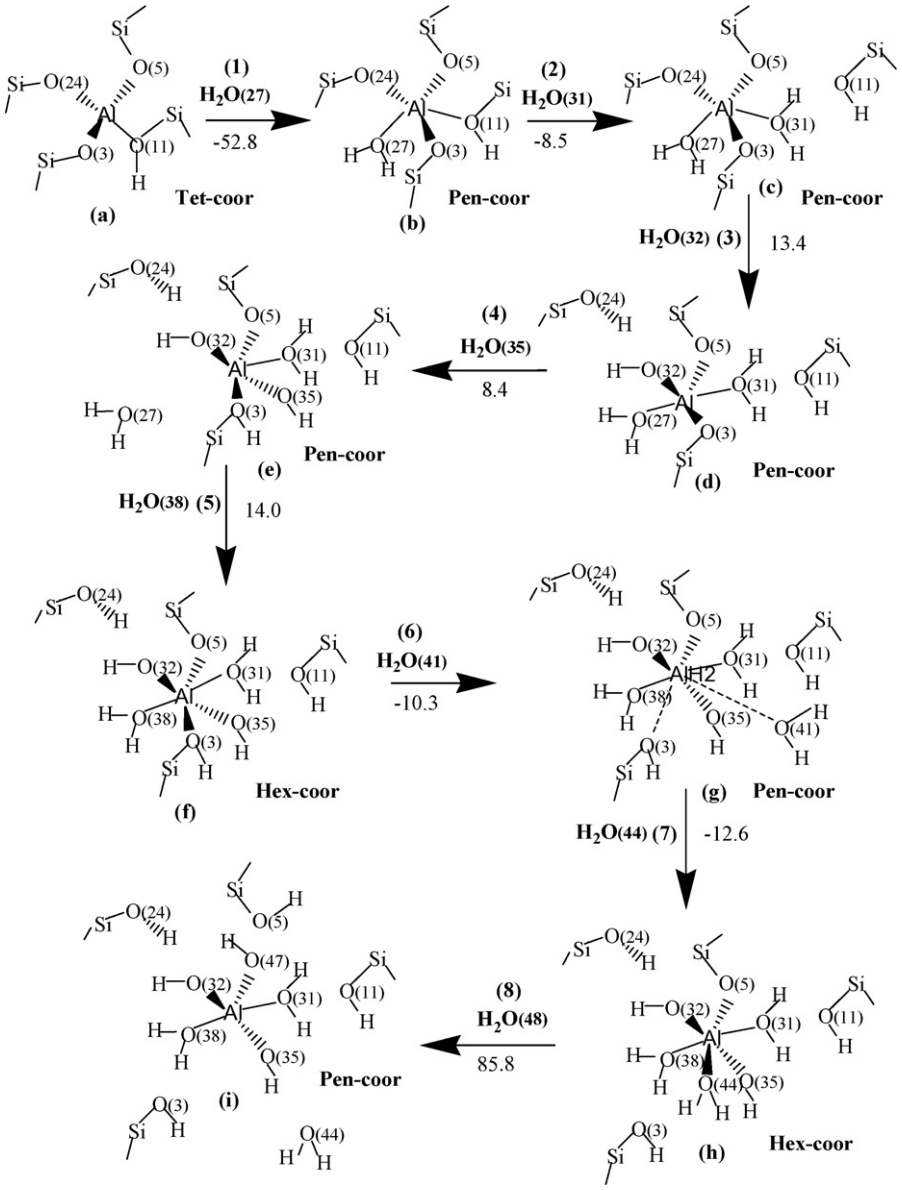

Fig. 4. Scheme of framework dealumination process for the $AlSi_{63}O_{152}H_{49}$ model.

approaching is limited by hindrance effects of other rings around the fourfold one.

As in the previous cluster, successive attacks of water molecules to the Al–O–Si bonds are considered. In the first step (see scheme shown in Fig. 4) the ($H_2O(27)$ interaction leads to a penta-coordinated aluminum atom (Fig. 4b), as in the previous model. Table 4 results indicate a relatively weak Al–O(27) bond formation with BD = 2.16 Å and a WI of 0.19. Once again, a bond strength weakening occurs in the Al–O(11) bond. In this respect, Jentys et al. [45], studying the HZSM5 adsorption sites, have found out that water adsorption affects primarily the bridged hydroxyl bonds. On the other hand, Kunkeler et al. [14] has proposed partially hydrolyzed FAL as the precursor for the catalytic active species in the steamed zeolite-beta. The process seems to be exothermic, although in this case the absolute value is higher (ΔDBE = −52.8 kcal/mol) than in the $AlSi_3O_{12}H_9$ model (ΔDBE −37.0 kcal/mol).

In a similar way that in the small model case, a second water molecule ($H_2O(31)$) adsorption causes the Al–O(11) bond rupture (BD = 3.82 Å and WI = 0.00. Note that BD(Al–O(11)) = 3.82 Å is shorter than in the small model (BD = 4.73 Å) due to the cage effect. In addition, this second water is adsorbed by the Al–O(31)H_2 bond formation (BD = 2.06 and WI = 0.23) (see Fig. 4c). A similar energetic trend is also observed with a ΔDBE of −8.5 kcal/mol respect to −3.1 kcal/mol in the small model, see step (2) in Figs. 4 and 3.

The addition of a third water molecule ($H_2O(32)$) leads the water bond cleavage and the formation of Al–O(32)H and SiO(24)–H bonds in a way akin to a previous model. The formation of internal Si–O–H groups have been also confirmed by Yashima et al. [46] who proposed a hydroxy nest structure from clustering SiOH groups around the empty Al site. Values of BD = 1.79 and WI = 0.64 in Table 4 suggest the formation of a relatively strong Al–O(32) bond that has characteristics of an OH group. In addition, the Al–O(24) bond is broken, as shown in a BD of 3.17 Å. The resulting penta-coordinate Al complex is bonded to the zeolite framework by two Al–O–Si bonds (Fig. 4d). Similarly, the Al–O binding energy change shown in Table 4 and Fig. 4 is positive (13.4 kcal/mol) following the same trend of the small model (2.7 kcal/mol) (see Table 3).

In a fourth step, water ($H_2O(35)$) interaction with the Al site generates the removal of $H_2O(27)$ adsorbed in the first step. In addition, the $H_2O(35)$ molecule produces the Al–O(35)H bond and at the same time a H atom transfers to the O(3) atom forming a Al–(O(3)–H)–Si structure (see Fig. 4e). This step is not observed in the small cluster model. Values presented in Table 4 of BD(Al–O(27)) = 3.40 Å and BD(Al–O(35)) = 1.83 Å confirm the $H_2O(27)$ release and the Al–O(35)H bond formation, respectively. The Al–O(27) bond breaking occurs instead of Al–O(3) because the former bond strength (BD = 2.08 Å and WI = 0.23) is weaker than that of Al–O(3) (BD = 1.78 Å and WI = 0.64). Note that this step leads to a fairly weak Al–O(3) bond and a decrease in local Al–O bonds by 16.5 kcal/mol.

The interaction of a fifth water ($H_2O(38)$) produces the formation of a hexacoordinated species (see Fig. 4f). In this case the octahedral species is bonded through the framework by two Al–O–Si bridge bonds with two adsorbed water molecules and two OH groups. This is different to that found in the small model that

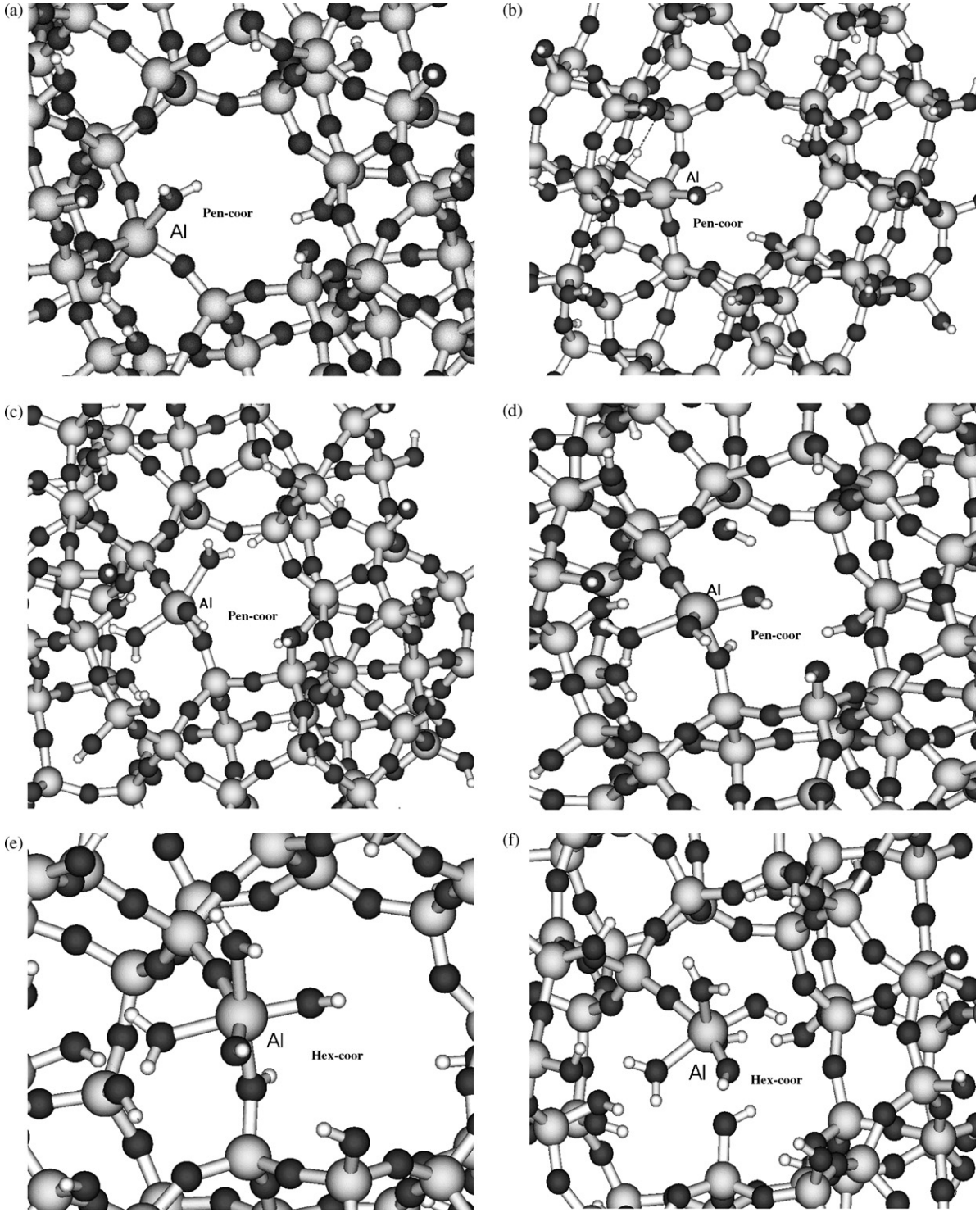

Fig. 5. Different species formed during the dealumination process. Dark balls go with O atoms, small white balls are H atoms, and gray balls correspond to Si atoms.

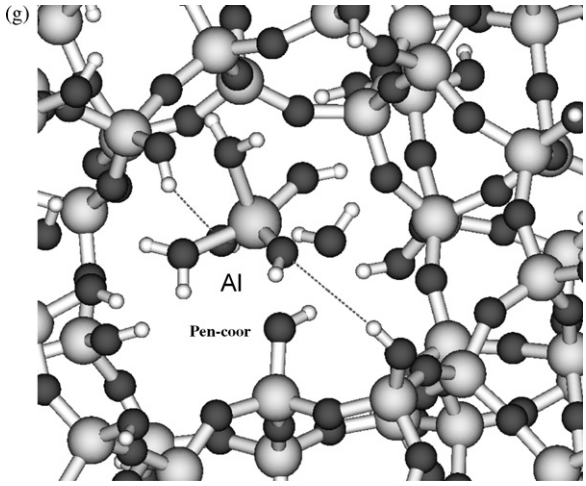

Fig. 5. (*Continued*).

has one single Al–O–Si bond (see Fig. 3f). As in previous cases, the H_2O adsorption causes an Al–O(3)H bond weakening, because the Al–O(3) bond distance increases from 1.98 to 2.13 Å.

After the addition of a sixth water ($H_2O(41)$) molecule an aluminum species evolves with one Al–O–Si bridge bond, two OH groups, and two coordinated H_2O. In addition, two very weak bonds are observed with BDs of 2.56 and 2.68 Å and with WIs of 0.11 and 0.05 for Al–O(3) and Al–O(41) bonds, respectively; see Fig. 4g and Table 4. This structure seems to have a sort of solvation shell by an interaction with a water molecule ($Al\cdots O(41)H_2$) and part of the framework ($Al\cdots O(3)HSi$). This step is locally favored by a ΔDBE of −10.2 kcal/mol.

The attack of other water molecule ($H_2O(44)$) (seventh step) will produces a complete Al–O(3) bond breaking, the slightly bonded $H_2O(41)$ release, and a $Al–O(44)H_2$ bond formation. This hexacoordinated intermediate has three H_2O and two OH groups bonded to the framework through one Al–Si–O bond, in a similar way to that found in the small cluster. Note that this step is locally favored with ΔDBE of −12.7 kcal/mol.

Finally the adsorption of $H_2O(47)$ (Fig. 4i) and Table 4) produces the Al–O(5) rupture between Al and the framework and the SiO(5)–H bond formation. The final EFAL has three OH groups and two H_2O molecules in a penta-coordinated species. These results agree with dynamical simulation carried out by Benco et al. [18] of six-coordinated cluster $Al(OH)_3(H_2O)_3$ in vacuo. The distances of Al–OH and $Al–OH_2$ obtained by Benco et al. are in the range of 1.74–1.78 Å and 2.05–2.14 Å that compares well with these results of 1.77–1.81 Å and 2.08–2.24 Å, respectively. However, Benco's work found that the Al atom coordination has three OH groups in the equatorial region and two axial H_2O, different from this work. Other agreement with these results was obtained by *ab initio* calculations of Ruiz et al. [19] for the tetrahedral to octahedral transformation coordinations in aluminum complexes. They found that a penta-coordinated complex is favored over the tetrahedral one and octahedral coordination and that six-coordinated species are not stable in the neutral state.

Comparison of the dealumination processes in the two models, $AlSi_3O_{12}H_9$ and $AlSi_{63}O_{152}H_{49}$, shows a similar behavior. The final EFAL complexes are different: $Al(OH)_3$ in the first case and $Al(OH)_3(H_2O)_2$ in the second one. The dissimilar environments around the Al are responsible of this difference. However, it is possible that $Al(OH)_3(H_2O)_2$ may lose water molecules all ends up in $Al(OH)_3$. This assertion is supported by experimental results obtained by Bugaev et al. [13], who reported the $Al(OH)_3$ formation at high temperatures or after cooling at room temperature under vacuum.

3.3. Models of intermediate species

The intermediate species generated during the EFAL formation are not completely known and here we present some of these obtained from modeling water interaction with zeolite models. Different species types are considered taking into account H_2O molecules, OH groups and Al–zeolite framework bond numbers.

The intermediate formation with one single H_2O molecule is highly probable because in both models it occurs. This intermediate species is penta-coordinate attached to the zeolite framework by four Al–O–Si bridge bonds, as shown in Fig. 5a. Note that the water adsorption from the straight channel is favored. The interaction of a second water molecule would lead to the formation of other penta-coordinate intermediate species in both models. Here the intermediate has three bonds to the zeolite framework and two water molecules attached, as depicted in Fig. 5b. Note that the water attack was from behind the straight channel and in an opposing direction of the previous adsorbed H_2O molecule. Other intermediate with two bonds to the framework is also formed in both models. It has two water molecules and one OH group bonded to the Al atom, as depicted in Fig. 5c, resulting in other penta-coordinated intermediate. This can be transformed in other penta-coordinated intermediate with two OH groups and one H_2O molecule (see Fig. 5d). Hexacoordinated intermediate, as shown in Fig. 5e, with two H_2O molecules and two OH groups, bonded to the framework by two bridge Si–O–Al bonds was found. Other hexacoordinated species with one framework bond was also observed. It has three H_2O molecules and two OH groups attached to the Al atom, as described in Fig. 5f. Finally, the free Al species is penta-coordinated with three OH groups and two H_2O molecules bonded to the Al atom, as presented in Fig. 5g. A further treatment of this unbonded species may lead to addition or loss of water molecules, yielding octahedral or tetrahedral and tricoordinated EFALs.

4. Conclusions and comments

Parametric method CATIVIC has been applied successfully to modeling the multifarious process of H-ZSM5 zeolite dealumination. The cost on time in relation to DFT methods is an indication of a promissory future for PQMs in modeling complicated processes

in complex systems. Theoretical modeling is very helpful in the recognition of intermediates that are very difficult to identify by experimental methods.

Several intermediate species were found in the dealumination process: penta-coordinated species with four, three, two and one bonds to the framework; and a hexacoordinated with two bonds with the framework.

The resulting EFAL in the dealumination process of H-ZSM5 zeolite are penta- ($Al(OH)_3(OH)_2$) or threefold ($Al(OH)_3$) coordinated species. Octahedral species are not discarded because these species are formed as intermediates in the EFAL formation. A SiOH nest is also produced in the framework.

Results support the fact that the dealumination is facilitated by acidified H_2O because the proton charge compensation weakens the Al–OHSi bonds. This feature would lead to intermediates with more H_2O bonded molecules than OH groups. Another possibility is the dissociation of H_2O molecules on Al–O–Si bonds to yield Al–OH plus SiO–H or AlO–H plus Si–OH. These last two mechanisms would produce intermediates with more OH groups than H_2O ligands.

More work has to be done considering the formation of positive charged intermediates and polymeric EFAL species. It means that water molecules and protons may react with the resulting species to produce more complex intermediates and EFAL compounds. In addition, several sites different to those located in the fourfold ring has to be considered. Van Bokhoven et al. [12] found that T1- and T2-sites in zeolite-beta, located in fourfold ring, are prevented to be dealuminated. Furthermore, it would be also important to include more than one water molecule to describe in a more realistic manner the stability of the formed species.

Acknowledgement

This work was supported by FONACIT, Venezuela, under the S1-2001000907 project for CATIVIC applications to zeolites.

References

[1] C. Marcilly, Oil & Gas Sci. & Tech. 56 (2001) 499.
[2] G. Centi, P. Ciambelli, S. Perathoner, P. Russo, Catal. Today 75 (2002) 3.
[3] J.D. Sherman, Proc. Natl. Acad. Sci. 96 (1999) 3471.
[4] A. Corma, M.J. Díaz-Cabañas, J. Martínez-Triguero, F. Rey, J. Rius, Nature 418 (2002) 514.
[5] P.V. Shertukde, W.K. Hall, J.-M. Dereppe, G. Marcelin, J. Catal. 139 (1993) 468.
[6] E. Bourgeat-Lami, P. Massiani, F. Di Renzo, P. Espiau, F. Fajula, Appl. Catal. 72 (1991) 139.
[7] X.Y. Lin, Y. Fan, Z.H. Liu, G. Shi, H.Y. Liu, X.J. Bao, Catal. Today 125 (2007) 185.
[8] J.P. Marques, I. Gener, P. Ayrault, J.C. Bordado, J.M. Lopes, F.R. Ribeiro, M. Guisnet, Comptes Rend. Chim. 8 (2005) 399.
[9] C. Jia, P. Massiani, D. Barthomeuf, J. Chem. Soc., Faraday. Trans. 89 (1993) 3659.
[10] M.J. Remy, D. Stanica, G. Poncelet, E.J.P. Feijen, P.J. Grobet, J.A. Martens, P.A. Jacobs, J. Phys. Chem. 100 (1996) 12440.
[11] A. Omegna, R. Prins, J.A. van Bokhoven, J. Phys. Chem. B. 109 (2005) 9280.
[12] J.A. van Bokhoven, D.C. Koningsberger, P. Kunkeler, H. van Bekkum, A.P.M. Kentgens, J. Am. Chem. Soc. 122 (2000) 12842.
[13] L.A. Bugaev, J.A. van Bokhoven, A.P. Sokolenko, Y.V. Latokha, L.A. Avakyan, J. Phys. Chem. B 109 (2005) 10771.
[14] P.J. Kunkeler, B.J. Zuurdeeg, J.C. van der Waal, J.A. van Bokhoven, D.C. Koningsberger, H. van Bekkum, J. Catal. 180 (1998) 234.
[15] X. Lin, Y. Fan, Z. Liu, G. Shi, H. Shi, H. Liu, X. Bao, Catal. Today 125 (2007) 185.
[16] V.I. Costa Vayá, P.G. Belelli, J.H.Z. dos Santos, M.L. Ferreira, D.E. Damiani, J. Catal. 204 (2001) 1.
[17] S. Li, A. Zheng, Y. Sul, H. Zhang, L. Chen, J. Yang, C. Ye, F. Deng, J. Am. Chem. Soc. 129 (2007) 11161.
[18] L. Benco, T. Demuth, J. Hafner, F. Hutschka, H. Toulhoat, J. Catal. 209 (2002) 480.
[19] J.M. Ruiz, M.H. McAdon, J.M. Garcés, J. Phys. Chem. B 101 (1997) 1733.
[20] D.L. Bhering, A. Ramírez-Solís, C.J.A. Mota, J. Phys. Chem. B 107 (2003) 4342.
[21] C.J.A. Mota, D.L. Bhering, N. Rosenbach, Angew. Chem. Int. Ed. 43 (2004) 3050.
[22] N. Rosenbach, C.J.A. Mota, Appl. Catal. A 336 (2008) 54.
[23] A.I. Biaglow, D.J. Parrillo, G.T. Kokotailo, R.J. Gorte, J. Catal. 148 (1994) 213.
[24] P. Lukinskas, D. Fărcaşiu, Appl. Catal. A 209 (2001) 193.
[25] F. Ruette, M. Sánchez, G. Martorell, C. González, R. Añez, A. Sierraalta, C. Mendoza, Int. J. Quantum Chem. 96 (2004) 321.
[26] Gaussian 98, Revision A. 11.4, M.J. Frisch, G.W. Trucks, H.B. Schlegel, G.E. Scuseria, M.A. Robb, J.R. Cheeseman, V.G. Zakrzewski, J.A. Montgomery, Jr., R.E. Ftatman, J.C. Burant, S. Dapprich, J.M. Millam, A.D. Daniels, K.N. Kudin, M.C. Strain, O. Farkas, J. Tomasi, V. Barone, M. Cossi, R. Cammi, B. Mennucci, C. Pomelli, C. Adamo, S. Clifford, J. Ochterski, G.A. Petersson, P.Y. Ayala, Q. Cui, K. Morokuma, N. Rega, P. Salvador, J.J. Dannenberg, D.K. Malick, A.D. Rabuck, K. Raghavachari, J.B. Foreman, J. Cioslowski, J.V. Ortiz, A.G. Baboul, B.B. Stefanov, G. Liu, A. Liashenko, P. Piskorz, I. Komaromi, R. Gomperts, R.L. Martin, D. Fox, T. Keith, M.A. Al-Laham, C.Y. Peng, A. Nanayakkara, M. Challacombe, P.M.W. Gill, B. Johnson, W. Chen, M.W. Wong, J.L. Andres, C. Gonzalez, M. Head-Gordon, E.S. Replogle, J.A. Pople, Gaussian, Inc., Pittsburgh, PA, 2002.
[27] M. Romero, M. Sánchez, A. Sierraalta, L. Rincón, F. Ruette, J. Chem. Inf. Comp. Sci. 39 (1995) 543.
[28] F. Ruette, C. Gonzalez, A. Octavio, J. Mol. Struct. (Theochem.) 537 (2001) 17.
[29] F. Ruette, S.A.M. Marcantognini, V.V. Karasiev, J. Mol. Struct. (Theochem.) 636 (2003) 15.
[30] R.C. Bingham, M.J. Dewar, D.H. Lo, J. Am. Chem. Soc. 97 (1975) 1285.
[31] M. Sánchez, R. Añez, A. Sierraalta, M. Rosa-Brussin, H. Soscun, F. Ruette, Ciencia 13 (2005) 94.
[32] K.B. Wiberg, Tetrahedron 24 (1968) 1083.
[33] (a) F. Ruette, F.M. Poveda, A. Sierraalta, J. Rivero, Surf. Sci. 349 (1996) 241; (b) F. Ruette, C. González, M. Sánchez, J. Mol. Struc. (Theochem.) 549 (2001) 9.
[34] www.IZA-structure.org/databases.
[35] G. Kresse, J. Furthmüller, Phys. Rev. B 54 (1996) 11169.
[36] F. Ruette, M. Sánchez, A. Sierraalta, C. Mendoza, R. Añez, L. Rodríguez, O. Lisboa, J. Daza, P. Manrique, Z. Perdomo, M. Rosas-Brussin, J. Mol. Catal. A: Chem. 228 (2005) 211.
[37] A.W. O'Donovan, C.T. O'Connor, K.R. Koch, Micropor. Mater. 5 (1995) 185.
[38] J.A. van Bokhoven, H. Sambe, D.E. Ramaker, D.C. Koningsberger, J. Phys. Chem. B 103 (1999) 7557.
[39] J.T. Miller, P.D. Hopkins, B.L. Meyers, G.J. Ray, R.T. Roginski, G.W. Zajac, N.H. Rosenbaum, J. Catal. 138 (1992) 115.
[40] I. Kiricsi, C. Flego, G. Pazzuconi, W.O. Parker Jr., R. Millini, C. Perego, G. Bellussi, J. Phys. Chem. 98 (1994) 4627.
[41] B.H. Wouters, T.H. Chen, P.J. Grobet, J. Am. Chem. Soc. 120 (1998) 11419.
[42] L.C. de Ménorval, W. Buckermann, F. Figueras, F. Fajula, J. Phys. Chem. 100 (1996) 465.
[43] J. Scherzer, ACS Symp. Series 248 (1984) 157.
[44] T.H. Fleisch, G.J. Ray, B.L. Meyers, C.L. Marshall, J. Catal. 99 (1986) 117.
[45] A. Jentys, G. Warecka, M. Derewinski, J.A. Lercher, J. Phys. Chem. 93 (1989) 4837.
[46] P. Wu, T. Komatsu, T. Yashima, J. Chem. Soc., Faraday Trans. 92 (1996) 861.